DOI: 10.1002/asia.201500234

Metal–Organic Frameworks

Metal-Ion Metathesis and Properties of Triarylboron-Functionalized Metal–Organic Frameworks

Xiaoqing Wang,[b] Liangliang Zhang,[a] Jie Yang,[b] Fangna Dai,[a] Rongming Wang,[a] and Daofeng Sun*[a, b]

Abstract: An anionic metal–organic framework, $H_3[(Mn_4Cl)_3\mathbf{L}_8]\cdot 30\,H_2O\cdot 2.5\,DMF\cdot 5\,Diox$ (**UPC-15**), was successfully prepared by the reaction of $MnCl_2$ with tris(*p*-carboxylic acid)tridurylborane ($H_3\mathbf{L}$) under solvothermal conditions. **UPC-15** with wide-open pores (~18.8 Å) is constructed by packing of octahedral and cuboctahedral cages, and exhibits high gas-sorption capabilities. Notably, **UPC-15** shows selective adsorption of cationic dyes due to the anion framework. Moreover, the catalytic and magnetic properties were investigated, and **UPC-15** can highly catalyze the cyanosilylation of aromatic aldehydes. **UPC-15** exhibits the exchange of metal ions from Mn to Cu in a single-crystal-to-single-crystal manner to generate **UPC-16**, which could not be obtained by the direct solvothermal reaction of $CuCl_2$ and $H_3\mathbf{L}$. **UPC-16** exhibits similar properties for gas sorption, dye separation, and catalytic activity. However, the magnetic behaviors for **UPC-15** and **UPC-16** are distinct due to the metal-specific properties. Below 47 K, **UPC-15** exhibits a ferromagnetic coupling but **UPC-16** shows a dominant antiferromagnetic behavior.

Introduction

Organic dyes are widely used in many industries, such as textile, paper, printing, cosmetics, and pharmaceutical industries. However, the emission of dyes contains some toxic contaminants, interferes with gas solubility in water, and inhibits the growth of aquatic biota.[1] Thus, scavenging dyes from waste water is a significant task. So far, various physical, chemical, and biological approaches have been proposed.[2] Among them, adsorption as one of the most feasible technologies has been used to remove dyes from contaminated water due to its effectiveness and economic competitiveness. The well-known adsorbents mainly include zeolites, carbons, and polymeric materials, which can effectively adsorb multiple mixed organic dye pollutants, but are difficult to selectively separate the targeted organic dyes.[3] Metal–organic frameworks (MOFs) with extra-large surface area have received considerable attention, as they exhibit the potential to impact technologies for catalysis, luminescence, gas storage and separation, magnetism, and other applications.[4–8] Due to tunable pore sizes and intriguing topological structures, MOFs are good candidates for selective separation of organic dyes.[9] On the one hand, MOFs can be used to separate dyes with different size, based on the size-exclusion effect via reasonable adjusting pore sizes.[10] On the other hand, ionic MOFs have more unique advantages on selective adsorption of cationic or anionic dyes due to guest–guest exchange interactions or host–guest electronic interactions.[11] However, in most cases, selective separation of organic dyes is mainly based on the size-exclusion effect. Thus, it is vital to design and synthesize ionic MOFs that can be used to selectively separate organic dye molecules by virtue of ionic selectivity.

Generally, MOFs are obtained by a one-pot synthesis (hydro/solvothermal), but this strategy lacks control and requires a trial and error to obtain predictable structures and excellent properties.[12] Recently, the post-synthetic modification (PSM) has gathered considerable attention as a viable option to prepare new analogues of porous MOFs. Compared with the direct synthesis, PSM can give a better control over the desired structures. Various PSM processes have been reported, which mainly include solvent-assisted linker exchange, non-bridging ligand replacement, transmetalation, or metal–ion exchange.[13] Among them, metal–ion exchange as a simple and effective method has been successfully used to synthesize MOFs with desired metal ions that are inaccessible through direct methods. Due to the incorporation of desired metal ions, the resulting MOFs could exhibit some desired functional behaviors, such as gas sorption, high stability, magnetism, ionic conductivity, and mediating site-isolated chemistry.[14] Although a synthetic pathway has been employed in some successful cases,

[a] *L. Zhang, F. Dai, Prof. R. Wang, Prof. D. Sun*
State Key Laboratory of Heavy Oil Processing
College of Science
China University of Petroleum (East China)
Qingdao, Shandong, 266580 (P.R. China)
E-mail: dfsun@upc.edu.cn

[b] *X. Wang, J. Yang, Prof. D. Sun*
Key Lab of Colloid and Interface Chemistry, Ministry of Education
School of Chemistry and Chemical Engineering
Shandong University
Jinan, Shandong, 250100 (P.R. China)

Supporting information for this article is available on the WWW under http://dx.doi.org/10.1002/asia.201500234.

more studies are needed to further understand various fundamental aspects that govern some unique chemical transformations.

In our previous work, we showed that the porosity and catalytic capacity of an MOF can be improved significantly through metal–ion metathesis.[14f] Herein, we report the metal-ion metathesis in a triarylboron-functionalized Mn^{II} MOF (**UPC-15**) based on a chloro-bridged square-planar tetrametallic cluster as the secondary building unit (SBU), generating a Cu^{II}/Mn^{II} MOF (**UPC-16**) due to incomplete metal-ion metathesis. The properties of the materials (**UPC-15** and **UPC-16**) including gas uptake, adsorption of dye molecules, catalysis, and magnetism were fully studied and compared. Significantly, both **UPC-15** and **UPC-16** exhibit selective adsorption of cationic dye molecules over anionic and neutral ones due to their anionic frameworks. Interestingly, when Mn ions were partly replaced by Cu ions, its magnetic property transforms from a ferromagnet to an antiferromagnet below 47 K. However, other properties changed only slightly with the metal-ion exchange.

Results and Discussion

Synthesis and crystal structure of UPC-15

Crystals of $H_3[(Mn_4Cl)_3\mathbf{L}_8]\cdot 30H_2O\cdot 2.5DMF\cdot 5Diox$ (**UPC-15**) were obtained by the reaction of $MnCl_2\cdot 6H_2O$ with $H_3\mathbf{L}$ in a mixture of DMF, 1,4-dioxane, and water at 95 °C for 50 h. Single-crystal X-ray determination reveals that **UPC-15** crystallizes in the cubic space group P_{432} and possesses an anionic 3D porous framework based on a μ_4-Cl-bridged square-planar $[Mn_4Cl]^{7+}$ SBU (Figure 1a). To balance the charge of the framework, three hydrogen ions per formula unit were suggested by elemental analysis. All Mn^{2+} ions are five-coordinated in a square pyramidal geometry, completed by a central chlorine atom, and four oxygen atoms from the carboxylate groups. The average distances of Mn–Cl and Mn–O are 2.329 Å and 2.187 Å, respectively. Each $[Mn_4Cl]^{7+}$ unit is surrounded by eight $\mathbf{L}^{3-}$ ligands. Meanwhile, each $\mathbf{L}^{3-}$ ligand connects three $[Mn_4Cl]^{7+}$ moieties to form a (8, 3)-connected net (Figure 1e). Overall, six square-planar $[Mn_4Cl]^{7+}$ units at the corners and eight planar $\mathbf{L}^{3-}$ ligands on the faces define octahedral cages, which are connected together through the vertices to generate cuboctahedral open cages (Figure 1b and 1c). The open cages are further interconnected to form 3D open channels with a diameter of 18.8 Å (atom-to-atom distance) (Figure 1d). The void space calculated using PLATON is approximately 55.0%, which is occupied by disordered solvent molecules.[15] Thermogravimetric analysis (TGA) of **UPC-15** indicates that the solvent molecules are removed from 20 °C to 298 °C, and then the complex starts to decompose (Figure S1, Supporting Information). Additionally, the IR spectrum and the powder XRD diffraction for **UPC-15** were also measured to verify its structure and the phase purity (Figures S2 and S3, Supporting Information).

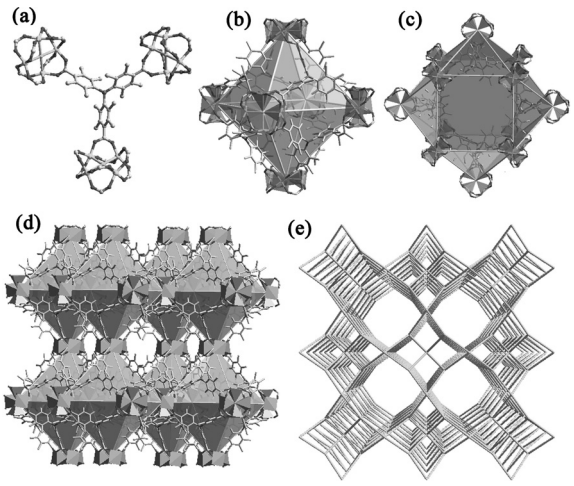

Figure 1. (a) Coordination environment of Mn^{II} ions in **UPC-15** and the linkage mode of $H_3\mathbf{L}$. (b) The octahedral cage. (c) The cuboctahedral cage. (d) The 3D packing of **UPC-15**. (e) Schematic representations of a simplified 3D network for **UPC-15**.

Post-synthetic modification via metal-ion metathesis

A solid-state post-synthetic modification as a novel synthetic strategy has been used to synthesize isomorphous MOFs with different metal ions, which are hard to obtain via conventional solvothermal reactions. Here, we tried to synthesize the isostructure of **UPC-15** with Cu ions via metal-ions metathesis, and the analogous framework **UPC-16** was obtained simply by soaking **UPC-15** in a solution of $CuCl_2$ in DMF for 15 days. The color of the crystals gradually turned green, indicating the substitution of the Cu ions (Figure 2b). To further confirm the metal-ion exchange reaction, inductively coupled plasma–atomic emission spectrometry (ICP–AES) and energy-dispersive X-ray spectroscopy (EDX) measurements were carried out (Figure 2c and 2d). Figure 2c shows that the metal-ion exchange rate is fast within the first 24 h and then becomes slow. The

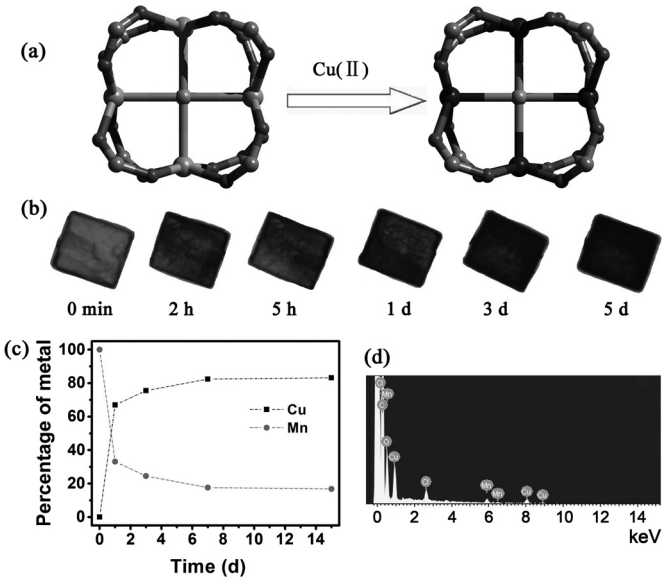

Figure 2. (a) Exchange of central metal ions at the SBUs. (b) Photos of a single crystal of **UPC-15** during immersion in a DMF solution of $CuCl_2$ (0.1 M) for different periods of time. (c) Kinetic profile of the Mn/Cu exchange process. (d) EDX spectra of **UPC-15** after immersion in a $CuCl_2$ solution for 5 days.

Mn^{2+} ions in **UPC-15** could not be completely exchanged by Cu^{2+} ions. An exchange of 83.2% of Mn by Cu was established by ICP–AES analysis after 15 days. On the basis of the ICP–AES analysis, the formula of **UPC-16** is $H_3[(Cu_{3.33}Mn_{0.67}Cl)_3L_8]$. The powder X-ray diffraction (PXRD) patterns indicated that **UPC-15** and **UPC-16** have the same crystalline structure (Figure S3). Furthermore, the single-crystalline nature of **UPC-16** can be confirmed by the single-crystal X-ray diffraction data, which revealed that **UPC-16** is isomorphous with **UPC-15** and exhibits the same SBU (Figure 2a). Thus, the outcome reveals that a single-crystal-to-single-crystal transformation occurred during the metal-ion metathesis. It is well known that the metal-exchange mechanism of MOFs includes two dominant factors: the coordination geometry and the coordination stabilities between the ligands and the central metal atoms. Since Mn^{2+} and Cu^{2+} usually exhibit similar coordination modes,[14c,e] no extra energy is required to overcome changes in configuration in the Mn/Cu exchange process. The Mn^{2+} ions are gradually exchanged with Cu^{2+} ions, and the ratio of Mn^{2+} and Cu^{2+} reaches finally a balance.[16]

Gas-uptake properties

Within the large octahedral cages and cuboctahedral open cages, both **UPC-15** and **UPC-16** possess considerable void space. To investigate their permanent porosities, the gas isotherms were measured for N_2, H_2, CO_2 and CH_4 at various temperatures. The samples were activated at different temperatures, and then the N_2 sorption isotherms were measured (Figure 3). It is found that the optimal activation temperatures for **UPC-15** and **UPC-16** are 40 °C and 80 °C, respectively, where they exhibit larger N_2-adsorption capacities. Accordingly, **UPC-15** and **UPC-16** were activated at 40 °C and 80 °C, respectively, for the following gas sorption measurements. Their N_2 adsorption isotherms correspond to typical type-I isotherms, which suggests the retention of the microporous structures after removal of guest molecules. The BET and Langmuir surface areas for **UPC-16** (1409.8 $m^2 g^{-1}$ and 1601.8 $m^2 g^{-1}$) are slightly larger than those for **UPC-15** (1354.2 $m^2 g^{-1}$ and 1539.9 $m^2 g^{-1}$). The measured pore volumes for **UPC-15** and **UPC-16** are 0.6098 $cm^3 g^{-1}$ and 0.6078 $cm^3 g^{-1}$, which are smaller than the values (0.8417 $cm^3 g^{-1}$ and 0.7320 $cm^3 g^{-1}$) calculated from their X-ray crystal structure by PLATON.[17] The reduced pore volumes are possibly due to shrinkage of the frameworks after the removal of the guest molecules. The plots of pore-size distribution show that both frameworks have a similar pore size (Figure S4, Supporting Information). The N_2-adsorption capacities of **UPC-15** and **UPC-16** at 1 bar are 393 $cm^3 g^{-1}$ and 395 $cm^3 g^{-1}$, respectively, which are much higher than those for other MOFs based on triarylboron-functionalized ligands reported.[18]

Additionally, the adsorption isotherms for low-pressure H_2, CO_2 and CH_4 at various temperatures are also shown in Figure 4. They all exhibit classical reversible type-I isotherms. Desolvated **UPC-15** can adsorb 119 $cm^3 g^{-1}$ (1.06 wt%) of H_2 at 1 bar and 77 K, and up to 71 $cm^3 g^{-1}$ (0.63 wt%) at 1 bar and 87 K. The H_2 uptake capacity at 77 K is higher than that for the zeolite ZSM-5 (0.7 wt%) and some other microporous MOFs.[19] The isosteric heat (Q_{st}) of H_2 adsorption can be calculated by fitting the gas adsorption isotherms at 77 K and 87 K. Compared with **UPC-15**, compound **UPC-16** exhibits a higher H_2 uptake capacity at 77 K (131 $cm^3 g^{-1}$). Figure 4b shows the H_2 isosteric heat of adsorption (Q_{st}) for **UPC-15** and **UPC-16**. At the lowest coverage, the Q_{st} values for **UPC-15** and **UPC-16** have estimated values of 6.33 $kJ mol^{-1}$ and 6.14 $kJ mol^{-1}$, respectively, which surpass that of MOF-5 (5.2 $kJ mol^{-1}$) and MOF-177 (4.4 $kJ mol^{-1}$).[20] For **UPC-15**, the CO_2 and CH_4 adsorption capacities at 273 K and 1 atm are 49 $cm^3 g^{-1}$ and 14 $cm^3 g^{-1}$, respectively. The Q_{st} values for CO_2 and CH_4, calculated by fitting the gas adsorption isotherms at 273 K and 293 K, are 25 and 12 $kJ mol^{-1}$, respectively. For **UPC-16**, the CO_2 and CH_4 adsorption capacities at 273 K and 1 atm are nearly identical to those for **UPC-15**, with total adsorption amounts of 48 $cm^3 g^{-1}$ and 16 $cm^3 g^{-1}$, respectively. However, the Q_{st} values are lower than those for **UPC-15**. These results are consistent with previously reported results.[14e]

Host–guest systems

Considering the large channels and anionic frameworks of **UPC-15** and **UPC-16**, we used these materials to adsorb and separate dye molecules from DMF solutions by virtue of ionic selectivity. Here, four dyes with different sizes and charges were chosen, including a neutral dye (solvent yellow 2), a cationic dye (methyl orange), and two anionic dyes (methylene blue and crystal violet). The dimensions of methylene blue and crystal violet were determined by using the MOPAC 7 software; they are 14.23 Å × 5.62 Å and 12.53 Å × 12.53 Å, respectively.[21] Obviously, they are all smaller than the pore size of **UPC-15** (18.8 Å), thus ensuring that the dye molecules can access its pores. The capabilities of **UPC-15** and **UPC-16** to capture dyes can be monitored by UV/Vis absorption spectroscopy. As shown in Figure 5a and 5b, when **UPC-15** was soaked in the mixed dye solutions of methylene blue/solvent yellow 2 and crystal violet/methyl orange, respectively, methylene blue and crystal violet can be effectively incorporated over

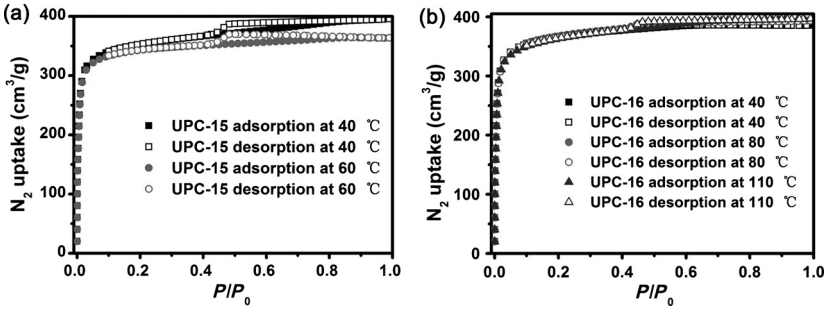

Figure 3. The N_2 sorption isotherms at 77 K for **UPC-15** (a) and **UPC-16** (b) at different activation temperatures.

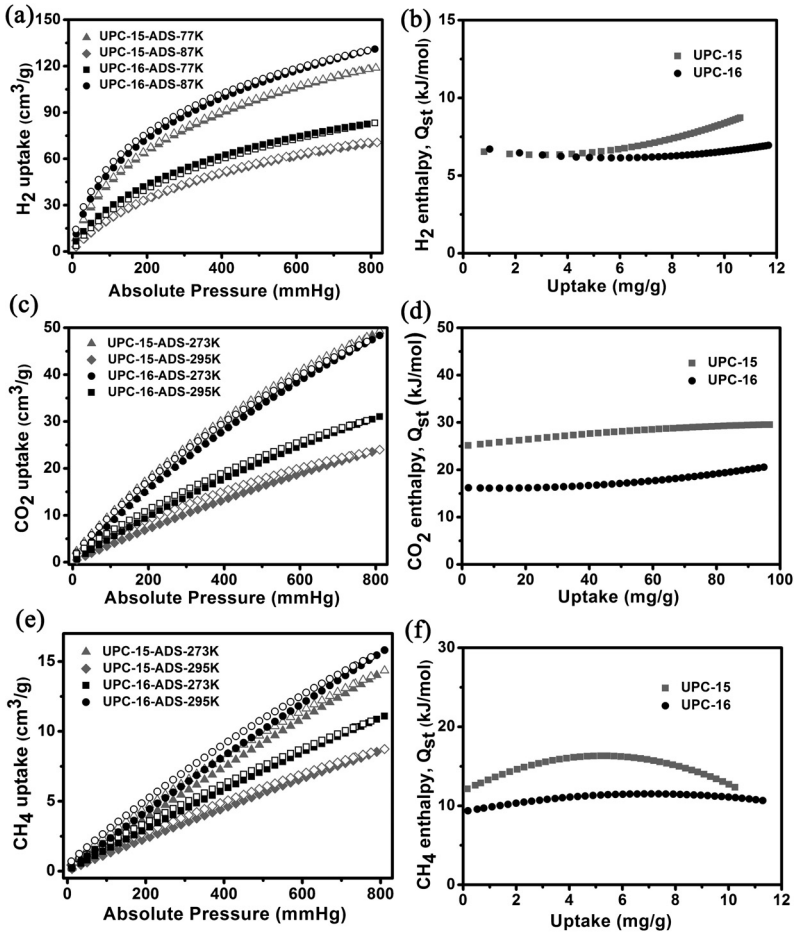

Figure 4. H_2, CO_2, and CH_4 sorption isotherms and isosteric heats of adsorption for **UPC-15** and **UPC-16**. Closed symbols, adsorption isotherms; open symbols, desorption isotherms.

a period of time, whereas the other dye molecules cannot be adsorbed. Moreover, the UV/Vis absorption spectra of solid **UPC-15** before and after soaking in the dye solution show the characteristic absorption peaks of dyes, which also suggests that methylene blue and crystal violet are incorporated into the network (Figure S5, Supporting Information). The sizes of methylene blue and crystal violet are much larger than those of solvent yellow 2 and methyl orange. The data indicated that **UPC-15** can effectively incorporate cationic dyes but not anionic and neutral dyes, which is attributed to the anionic framework of **UPC-15**. The cations in the network can be exchanged with cationic dye molecules. Due to the same structure and pore volume, **UPC-16** exhibits a similar phenomenon (Figure 5c and 5d). These results indicate that the anionic frameworks of **UPC-15** and **UPC-16** are responsible for the selective adsorption of cationic dyes with different sizes.

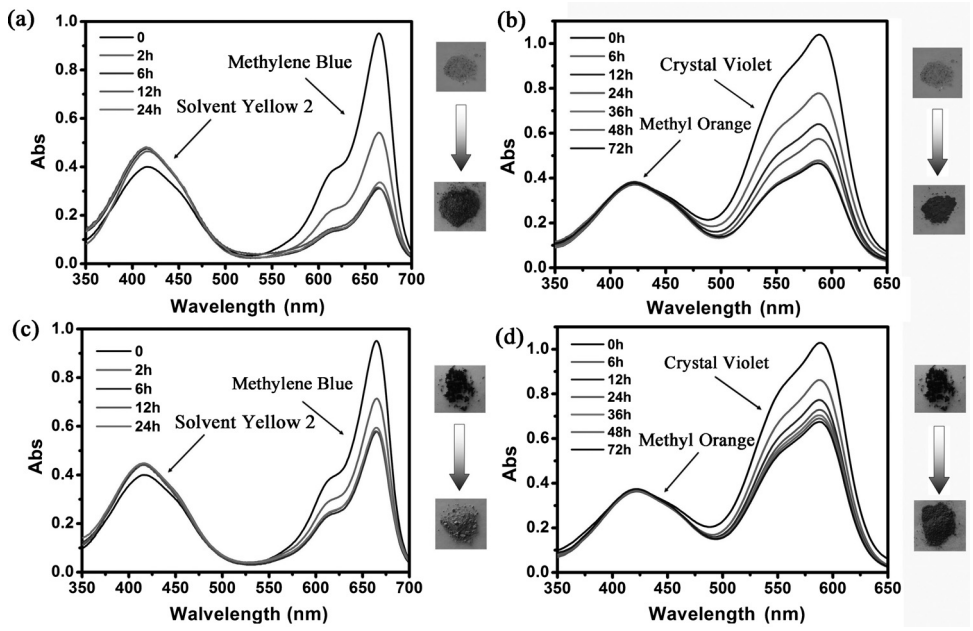

Figure 5. The UV/Vis spectra of the dye solutions with **UPC-15** (top) and **UPC-16** (bottom). a,c) Solvent yellow 2 and methylene blue. b,d) Methyl orange and crystal violet.

Cyanosilylation of aromatic aldehydes

Since the 18.8 Å pores of **UPC-15** and **UPC-16** are readily accessible and present a surface with coordinatively unsaturated metal sites, the large guest molecules that enter the framework pores can interact with the Lewis acidic metal sites, suggesting that **UPC-15** and **UPC-16** can act as heterogeneous catalysts for the catalytic conversion of organic substrates. The BET surface areas for **UPC-15** and **UPC-16** were obtained by the measurement of N_2 adsorption, and they are 1354.2 $m^2 g^{-1}$ and 1409.8 $m^2 g^{-1}$, respectively. Desolvated **UPC-15** and **UPC-16** were tested in the cyanosilylation of aromatic aldehydes. Catalyst (0.078 mmol%) was added

Table 1. Results for the cyanosilylation of aldehyde substrates in the presence of compounds **UPC-15** and **UPC-16**.

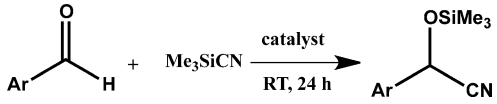

Entry	Catalyst	Ar	Yield [%]
1	**UPC-15**	phenyl	99.0
2	**UPC-15**	4-fluorophthyl	100
3	**UPC-15**	4-*tert*-butylphenyl	96.3
4	**UPC-16**	phenyl	97.1
5	$MnCl_2$	phenyl	77.8
6	$CuCl_2$	phenyl	69.3

to a mixture of aldehyde (0.5 mmol) and trimethylsilyl cyanide (1 mmol), and subsequently the mixture was stirred under a nitrogen atmosphere for 24 h at room temperature. The product yields were then determined by GC-MS and are shown in Table 1. For **UPC-15**, the conversion of benzaldehyde reaches 99.0%, which is fairly high compared to the conversion achieved in the presence of other MOFs.[22] Additionally, an excellent result was obtained for *p*-fluorobenzaldehyde (100% conversion), and the conversion of *p*-tertbutyl benzaldehyde was also a staggering 96.3%. The slightly lower conversion of *p*-tertbutyl benzaldehyde may be attributed to a size-selectivity effect. To investigate the metal ion-dependent variation of the conversion, desolvated **UPC-16** was tested in the cyanosilylation of benzaldehyde, and the conversion reached 97.1%, a value slightly lower than that for catalyst **UPC-15**. This is possibly due to the fact that a smaller ionic radius leads to stronger steric interactions of the substrates which approach the coordinatively unsaturated metal ions in the framework.[22b] Compared with the inorganic salts ($MnCl_2$ and $CuCl_2$), **UPC-15** and **UPC-16** exhibit a much higher catalytic activity (Table 1).

Magnetic studies

Magnetic properties for crystalline samples of **UPC-15** and **UPC-16** were measured under a field of 1000 Oe in the temperature range 1.8–300 K. The plots of $\chi_M T$ versus T for **UPC-15** and **UPC-16** are shown in Figure 6. For **UPC-15**, the $\chi_M T$ value at room temperature is about 14.05 $cm^3 mol^{-1} K$, which is much lower than the spin-only value of 17.5 $cm^3 mol^{-1} K$ for four uncoupled spin Mn^{II} ions ($S=5/2$, $g=2.0$). The $\chi_M T$ product continually decreases to a minimum of about 9.09 $cm^3 mol^{-1} K$ at 43.07 K, subsequently increases rapidly to a maximum of 16.92 $cm^3 mol^{-1} K$ at 31.78 K, and finally descends sharply on further cooling. It is obvious that **UPC-15** exhibits antiferromagnetic behavior above 43.07 K owing to the Boltzmann population of the ground state and depopulation of the excited states. The sharp increase below 43 K indicates a ferromagnetic coupling due to spin-canting or canted antiferromagnetism. A similar phenomenon was reported previously.[23] The magnetic susceptibility above 100 K abides by the Curie–Weiss law, $\chi = C/(T-\theta)$, with $C = 16.39\ cm^3$ and $\theta = -49.89$ K (Figure S6, Supporting Information). Compared with **UPC-15**, compound **UPC-16** exhibits distinct magnetic properties. The $\chi_M T$ value of 2.94 $cm^3 mol^{-1} K$ at room temperature is lower than the spin-only value of 4.18 $cm^3 mol^{-1} K$ for 3.33 Cu^{II} and 0.67 Mn^{II} ions (assuming $S_{Cu}=1/2$, $S_{Mn}=5/2$, and $g_{Cu}=g_{Mn}=2.0$). As shown in Figure 6, the $\chi_M T$ product decreases smoothly, suggesting a dominant antiferromagnetic coupling. The susceptibility data obeys the Curie–Weiss law above 100 K with $C = 3.79\ cm^3$ and $\theta = -74.17$ K (Figure S6). The differences in the magnetic properties for **UPC-15** and **UPC-16** are attributed to the metal-ion change of the framework.

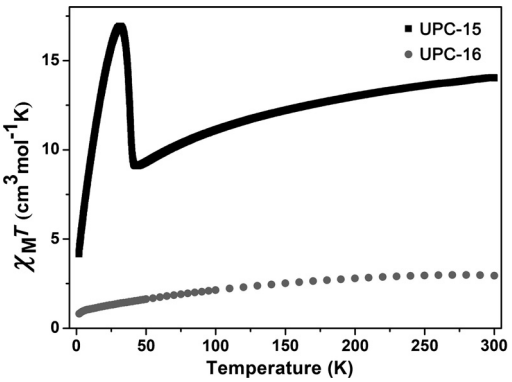

Figure 6. The magnetic susceptibility plot of $\chi_M T$ versus T for **UPC-15** and **UPC-16**.

Conclusions

In conclusion, an anionic Mn MOF (**UPC-15**) was successfully prepared based on a tris(*p*-carboxylic acid)tridurylborane (H_3**L**) ligand under solvothermal conditions. It is constructed by packing of octahedral cages and cuboctahedral open cages and has wide-open pores (~18.8 Å). Through metal-ion metathesis, Mn^{2+} ions can be partly exchanged by Cu^{2+} ions in a single-crystal-to-single-crystal manner to generate **UPC-16**, which cannot be directly synthesized by a solvothermal reaction of Cu^{2+} and H_3**L**. Both **UPC-15** and **UPC-16** exhibit selective adsorption of cationic dye molecules due to their anionic frameworks, which is different from the separation of dyes based on the size-exclusion effect. Magnetic measurements revealed that the magnetic behaviors for **UPC-15** and **UPC-16** are distinctly different. Below 47 K, **UPC-15** exhibits a ferromagnetic coupling while **UPC-16** shows a dominant antiferromagnetic behavior, which is attributed to the metal-specific properties.

Experimental Section

Synthesis of UPC-15 $H_3[(Mn_4Cl)_3L_8]\cdot 30H_2O\cdot 2.5DMF\cdot 5Diox$: $MnCl_2\cdot 4H_2O$ (2.0 mg, 0.010 mmol) and H_3**L** (1.0 mg, 0.0026 mmol) were dissolved in 1 mL mixed solution of DMF/1,4-dioxane/H_2O (5/2/1) and heated to 95 °C for 50 h in a sealed tube. The resulting brown crystalline blocks were collected by filtration, washed with DMF and EtOH, and dried in air (yield: 25%). Elemental analysis calcd (%) for **UPC-15**: C 56.0, H 6.54, N 0.56; found: C 57.2, H 6.51, N 0.54. IR (KBr): $\tilde{\nu} = 3411$ (s), 3221 (w), 1628 (s), 1427 (w), 1282 (w), 1094 (w), 859 (w), 625 (m), 480 (w), 392 cm^{-1} (w).

Synthesis of UPC-16 $H_3[(Cu_{3.33}Mn_{0.67}Cl)_3L_8]\cdot 30\,H_2O\cdot 9\,DMF\cdot 4\,Diox$: In a typical metal-ion exchange experiment, the crystals of as-synthesized **UPC-15** were immersed in a DMF solution of $CuCl_2\cdot 2\,H_2O$ (0.10 M) for 15 days, and the solvent was refreshed every three days. Subsequently, the metal-ion changed crystals were rinsed and soaked in DMF for 3 days. About 83.2% of Mn^{2+} ions were exchanged by Cu^{2+} ions, as assessed by inductively coupled plasma–atomic emission spectrometry (ICP–AES) analysis. Elemental analysis calcd (%) for **UPC-16**: C 54.8, H 6.64, N 1.87; found: C 55.3, H 6.58, N 1.65. IR (KBr): $\tilde{\nu}=3439$ (s), 2929 (w), 1653 (s), 1545 (m), 1427 (m), 1273 (w), 1101 (w), 866 (w), 631 (w), 421 cm^{-1} (w).

Acknowledgements

This work was supported by the NSFC (Grant Nos. 21271117, 21371179), NCET-11-0309, NSF of Shandong Province (BS2011L041), and the Fundamental Research Funds for the Central Universities (13CX05010A, 13CX02006A).

Keywords: catalytic · gas adsorption · magnetic propterties · metal-ions exchange · metal–organic frameworks · selective dye adsorption

[1] a) B. Adhikari, G. Palui, A. Banerjee, *Soft Matter* **2009**, *5*, 3452 – 3452; b) M. A. Al-Ghouti, M. Khraisheh, S. J. Allen, M. N. Ahmad, *J. Environ. Manage.* **2003**, *69*, 229 – 238; c) L. Zhou, C. Gao, W. Xu, *ACS Appl. Mater. Interfaces* **2010**, *2*, 1483 – 1491.

[2] a) A. Mittal, A. Malviya, D. Kaur, J. Mitta, L. Kurup, *J. Hazard. Mater.* **2007**, *148*, 229 – 240; b) B. Y. Shi, G. H. Li, D. S. Wang, C. H. Feng, H. X. Tang, *J. Hazard. Mater.* **2007**, *143*, 567 – 574; c) W. X. Chen, W. Y. Lu, Y. Y. Yao, M. H. Xu, *Environ. Sci. Technol.* **2007**, *41*, 6240 – 6245.

[3] a) Y. C. Wong, Y. S. Szeto, W. H. Cheung, G. Mckay, *Langmuir* **2003**, *19*, 7888 – 7894; b) Y. Al-Degs, M. A. M. Khraisheh, S. J. Allen, M. N. Ahmad, *Water Res.* **2000**, *34*, 927 – 935; c) C. K. Lee, S. S. Liu, L. C. Juang, C. C. Wang, K. S. Lin, M. D. Lyu, *J. Hazard. Mater.* **2007**, *147*, 997 – 1005.

[4] a) A. M. Shultz, O. K. Farha, J. T. Hupp, S. T. Nguyen, *J. Am. Chem. Soc.* **2009**, *131*, 4204 – 4205; b) J. Liu, L. Chen, H. Cui, J. Zhang, L. Zhang, C. Y. Su, *Chem. Soc. Rev.* **2014**, *43*, 6011 – 6061; c) H. Fei, J. Shin, Y. S. Meng, M. adelhardt, J. Sutter, K. Meyer, S. M. Cohen, *J. Am. Chem. Soc.* **2014**, *136*, 4965 – 4973.

[5] a) Y. J. Cui, Y. F. Yue, G. D. Qian, B. L. Chen, *Chem. Rev.* **2012**, *112*, 1126 – 1162; b) Z. Wei, Z. Y. Gu, R. K. Arvapally, Y. P. Chen, R. N. McDougald, A. A. Yakovenko, D. Feng, M. A. Omary, H. C. Zhou, *J. Am. Chem. Soc.* **2014**, *136*, 8269 – 8276; c) L. E. Kreno, K. Leong, O. K. Farha, M. Allendorf, R. P. V. Duyne, J. T. Hupp, *Chem. Rev.* **2012**, *112*, 1105 – 1125.

[6] a) L. J. Murray, M. Dincă, J. R. Long, *Chem. Soc. Rev.* **2009**, *38*, 1294 – 1314; b) H. C. Zhou, J. R. Long, O. M. Yaghi, *Chem. Rev.* **2012**, *112*, 673 – 674; c) M. P. Suh, H. J. Park, T. K. Prasad, D. W. Lim, *Chem. Rev.* **2012**, *112*, 782 – 835; d) K. Sumida, D. L. Rogow, J. A. Mason, T. M. McDonald, E. D. Bloch, Z. R. Herm, T. H. Bae, J. R. Long, *Chem. Rev.* **2012**, *112*, 724 – 781.

[7] a) M. Wriedt, A. A. Yakovenko, G. L. Halder, A. V. Prosvirin, K. R. Dunbar, H. C. Zhou, *J. Am. Chem. Soc.* **2013**, *135*, 4040 – 4050; b) L. Shen, S. W. Yang, S. C. Xiang, T. Liu, B. C. Zhao, M. F. Ng, J. Göttlicher, J. Yi, S. Li, L. Wang, J. Ding, B. L. Chen, S. H. Wei, Y. P. Feng, *J. Am. Chem. Soc.* **2012**, *134*, 17286 – 17290; c) C. Eugenio, M. E. Cuilermo, *Chem. Soc. Rev.* **2013**, *42*, 1525 – 1539.

[8] a) V. Stavila, A. A. Talin, M. D. Allendorf, *Chem. Soc. Rev.* **2014**, *43*, 5994 – 6010; b) K. M. L. Taylor-Pashow, J. D. Rocca, Z. G. Xie, S. Tran, W. B. Lin, *J. Am. Chem. Soc.* **2009**, *131*, 14261 – 14263; c) R. Ameloot, F. Vermoortele, W. Vanhove, M. B. J. Roeffaers, B. F. Sels, D. E. De Vos, *Nat. Chem.* **2011**, *3*, 382 – 387.

[9] J. R. Li, H. C. Zhou, *Nat. Chem.* **2010**, *2*, 893 – 898.

[10] a) F. Pu, X. Liu, B. L. Xu, J. S. Ren, X. G. Qu, *Chem. Eur. J.* **2012**, *18*, 4322 – 4328; b) Y. Q. Lan, H. L. Jiang, S. L. Li, Q. Xu, *Adv. Mater.* **2011**, *23*, 5015 – 5020; c) H. L. Jiang, Y. Tatsu, Z. H. Lu, Q. Xu, *J. Am. Chem. Soc.* **2010**, *132*, 5586 – 5587.

[11] a) C. Y. Sun, X. L. Wang, C. Qin, J. L. Jin, Z. M. Su, P. Huang, K. Z. Shao, *Chem. Eur. J.* **2013**, *19*, 3639 – 3645; b) C. Zou, Z. J. Zhang, X. Xu, Q. H. Gong, J. Li, C. D. Wu, *J. Am. Chem. Soc.* **2012**, *134*, 87 – 90; c) K. Gedrich, M. Heitbaum, A. Notzon, I. Senkovska, R. Fröhlich, J. Getzschmann, U. Mueller, F. Glorius, S. Kaskel, *Chem. Eur. J.* **2011**, *17*, 2099 – 2106.

[12] P. Deria, J. E. Mondloch, O. Karagiaridi, W. Bury, J. T. Hupp, O. K. Farha, *Chem. Soc. Rev.* **2014**, *43*, 5896 – 58912.

[13] a) O. Karagiaridi, M. B. Lalonde, W. Bury, A. A. Sarjeant, O. K. Farha, J. T. Hupp, *J. Am. Chem. Soc.* **2012**, *134*, 18790 – 18796; b) O. Karagiaridi, W. Bury, E. Tylianakis, A. A. Sarjeant, J. T. Hupp, O. K. Fatha, *Chem. Mater.* **2013**, *25*, 3499 – 3503; c) P. Deria, J. E. Mondloch, E. Tylianakis, P. Ghosh, W. Bury, R. Q. Snurr, J. T. Hupp, O. K. Farha, *J. Am. Chem. Soc.* **2013**, *135*, 16801 – 16804; d) P. Deria, W. Bury, J. T. Hupp, O. K. Farha, *Chem. Commun.* **2014**, *50*, 1965 – 1968; e) T. K. Prasad, D. H. Hong, M. P. Suh, *Chem. Eur. J.* **2010**, *16*, 14043 – 14050.

[14] a) Z. J. Zhang, W. Shi, Z. Niu, H. H. Li, B. Zhao, P. Cheng, D. Z. Liao, S. P. Yan, *Chem. Commun.* **2011**, *47*, 6425 – 6427; b) A. P. Nelson, O. K. Farha, K. L. Mulfort, J. T. Tupp, *J. Am. Chem. Soc.* **2009**, *131*, 458 – 460; c) M. Dincă, J. R. Long, *J. Am. Chem. Soc.* **2007**, *129*, 11172 – 11176; d) S. Das, H. Kim, K. Kim, *J. Am. Chem. Soc.* **2009**, *131*, 3814 – 3815; e) Y. Kim, S. Das, S. Bhattacharya, S. Hong, M. G. Kim, M. Yoon, S. Natarajan, K. Kim, *Chem. Eur. J.* **2012**, *18*, 16642 – 16648; f) J. Yang, X. Q. Wang, F. N. Dai, L. L. Zhang, R. M. Wang, D. F. Sun, *Inorg. Chem.* **2014**, *53*, 10649 – 10653; g) Z. Zhang, L. Zhang, L. Wojtas, P. Nugent, M. Eddaoudi, M. J. Zaworotko, *J. Am. Chem. Soc.* **2012**, *134*, 924 – 927; h) Z. Zhang, L. Wojtas, M. Eddaoudi, M. J. Zaworotko, *J. Am. Chem. Soc.* **2013**, *135*, 5982 – 5985; i) T. F. Liu, L. F. Zou, D. W. Feng, Y. P. Chen, S. Fordham, X. Wang, Y. Y. Liu, H. C. Zhou, *J. Am. Chem. Soc.* **2014**, *136*, 7813 – 7816; j) J. Zhao, L. Mi, J. Hu, H. Hou, Y. Fan, *J. Am. Chem. Soc.* **2008**, *130*, 15222 – 15223; k) L. Mi, H. Hou, Z. Song, H. Han, Y. Fan, *Chem. Eur. J.* **2008**, *14*, 1814 – 1821; l) L. Mi, H. Hou, Z. Song, H. Han, H. Han, H. Xu, Y. Fan, S.-W. Ng, *Cryst. Growth Des.* **2007**, *7*, 2553 – 2561.

[15] A. L. Spek, *Acta Crystallogr. Sect. A* **1990**, *46*, C34.

[16] W. Meng, H. Li, Z. Xu, S. Du, Y. Li, Y. Zhu, Y. Han, H. Hou, Y. Fan, M. Tang, *Chem. Eur. J.* **2014**, *20*, 2945 – 2952.

[17] A. L. Spek, *J. Appl. Crystallogr.* **2003**, *36*, 7 – 13.

[18] a) B. A. Blight, R. Guillet-Nicolas, F. Kleitz, R. Y. Wang, S. Wang, *Inorg. Chem.* **2013**, *52*, 1673 – 1675; b) X. Q. Wang, J. Yang, L. L. Zhang, F. L. Liu, F. N. Dai, D. F. Sun, *Inorg. Chem.* **2014**, *53*, 11206 – 11212.

[19] a) M. G. Nijkamp, J. E. M. J. Raaymakers, A. J. Van Dillen, K. P. De Jong, *Appl. Phys. A* **2001**, *72*, 619 – 623; b) D. Han, F. L. Jiang, M. Y. Wu, L. Chen, Q. X. Chen, M. C. Hong, *Chem. Commun.* **2011**, *47*, 9861 – 9863; c) J. L. C. Rowsell, O. M. Yaghi, *J. Am. Chem. Soc.* **2006**, *128*, 1304 – 1315; d) A. Dailly, J. J. Vajo, C. C. Ahn, *J. Phys. Chem. B* **2006**, *110*, 1099 – 1101; e) M. P. Suh, Y. E. Cheon, E. Y. Lee, *Chem. Eur. J.* **2007**, *13*, 4208 – 4215.

[20] a) S. Ma, H.-C. Zhou, *J. Am. Chem. Soc.* **2006**, *128*, 11734 – 11735; b) H. Furukawa, M. A. Miller, O. M. Yaghi, *J. Mater. Chem.* **2007**, *17*, 3197 – 3204.

[21] J. J. P. Stewart. MOPAC, A Semiempirical Molecular Orbital Program QCPE, **1983**, 455, version 6.0, **1990**.

[22] a) S. Horike, M. Dincă, K. Tamaki, J. R. Long, *J. Am. Chem. Soc.* **2008**, *130*, 5854 – 5855; b) M. Gustafsson, A. Bartoszewicz, B. Martín-Matute, J. L. Sun, J. Grins, T. Zhao, Z. Y. Li, G. S. Zhu, X. D. Zou, *Chem. Mater.* **2010**, *22*, 3316 – 3322; c) R. F. D'Vries, M. Iglesias, N. Snejko, E. Gutiérrez-Puebla, M. A. Monge, *Inorg. Chem.* **2012**, *51*, 11349 – 11355; d) R. Fernández de Luis, M. K. Urtiaga, J. L. Mesa, E. S. Larrea, M. Iglesias, T. Rojo, M. I. Arriortua, *Inorg. Chem.* **2013**, *52*, 2615 – 2626.

[23] a) R. A. Agarwal, A. Aijaz, C. Sañudo, Q. Xu, P. K. Bharadwaj, *Cryst. Growth Des.* **2013**, *13*, 1238 – 1245; b) Y. X. Liu, D. Liu, Y. Yu, J. Xu, X. H. Han, C. Wang, *CrystEngComm* **2013**, *15*, 10611 – 10617; c) F. L. Liu, L. L. Zhang, R. M. Wang, J. Sun, J. Yang, Z. Chen, X. P. Wang, D. F. Sun, *CrystEngComm* **2014**, *16*, 2917 – 2928.

Manuscript received: March 11, 2015
Accepted article published: April 30, 2015
Final article published: May 27, 2015